

## Microstructure and electrical properties of ZnO-Pr<sub>6</sub>O<sub>11</sub>-CoO-Cr<sub>2</sub>O<sub>3</sub>-Dy<sub>2</sub>O<sub>3</sub>-based varistor ceramics

CHOON-WOO NAHM, JONG-AH PARK, MYUNG-JUN KIM  
 Department of Electrical Engineering, Donggeui University, Busan 614-714, Korea  
 E-mail: cwnahm@donggeui.ac.kr

BYOUNG-CHUL SHIN  
 Department of Information and Materials Engineering, Donggeui University, Busan 614-714, Korea

ZnO varistors are electronic ceramic devices made by sintering ZnO powder with small amounts of various metal oxides, containing necessarily Pr<sub>6</sub>O<sub>11</sub> or Bi<sub>2</sub>O<sub>3</sub>. They exhibit highly nonlinear voltage-current (V-I) characteristics expressed by  $I = kV^\alpha$ , where  $k$  is a constant and  $\alpha$  is a nonlinear exponent, inherent parameter of varistors, and they possess excellent surge withstanding capabilities. Therefore, they have been extensively used to protect semiconductor devices, electronic circuits, and electric power systems from dangerous overvoltage [1, 2]. The majority of commercial ZnO varistors necessarily contain Bi<sub>2</sub>O<sub>3</sub> as varistor-forming oxides (VFO) and they exhibit excellent varistor properties. However, they have a few shortcomings due to the high volatility and reactivity of Bi<sub>2</sub>O<sub>3</sub> melted at about 825 °C during a sintering above 1000 °C [3]. The former changes varistor characteristics with the variation of inter-composition ratio of additives, the latter destroys the multi-layer structure of chip varistors, and it generates an insulating spinel phase deteriorating surge-absorption capabilities. Furthermore, they need many additives to obtain the high nonlinearity and stability.

In the past few years, ZnO varistor ceramics containing Pr<sub>6</sub>O<sub>11</sub> as VFO have been studied to overcome these problems [4–10]. In the former work, Nahm *et al.* reported that ZnO-Pr<sub>6</sub>O<sub>11</sub>-CoO-Cr<sub>2</sub>O<sub>3</sub>-M<sub>2</sub>O<sub>3</sub> ( $M = \text{Er, Y}$ )-based varistor ceramics exhibit high nonlinear properties and stability [6–10]. Many researchers who are interested in varistors wish to fabricate ZnO varistors exhibiting both higher nonlinearity and higher stability. It is very important to scrutinize the role of individual additive to apply ZnO-Pr<sub>6</sub>O<sub>11</sub>-based varistors in various areas. The purpose of this work is to investigate the effect of Dy<sub>2</sub>O<sub>3</sub> incorporation on microstructure and electrical properties of ZnO-Pr<sub>6</sub>O<sub>11</sub>-CoO-Cr<sub>2</sub>O<sub>3</sub>-Dy<sub>2</sub>O<sub>3</sub> (in short ZPCCD)-based varistors.

Reagent-grade raw materials were prepared for ZnO varistors with composition (98.0 -  $x$ ) mol% ZnO + 0.5 mol% Pr<sub>6</sub>O<sub>11</sub> + 1.0 mol% CoO + 0.5 mol% Cr<sub>2</sub>O<sub>3</sub> +  $x$  mol% Dy<sub>2</sub>O<sub>3</sub> ( $x = 0.0$ – $2.0$ ). After milling, the mixture was calcined in air at 750 °C for 2 h. The calcined powders were pressed into discs of 10 mm in diameter and 1.8 mm in thickness at a pressure of 80 MPa. The discs were sintered at 1350 °C in air for 1 h. The size of the final samples was about 8 mm in diameter and 1.0 mm in thickness. Silver paste was

coated on both faces of the samples and ohmic contacts were formed by heating at 600 °C for 10 min. The size of electrodes was 5 mm in diameter. The V-I characteristics of the varistors were measured using a Keithley 237 unit. The varistor voltage ( $V_{1\text{mA}}$ ) was measured at a current density of 1.0 mA/cm<sup>2</sup> and the leakage current ( $I_L$ ) was measured at 0.80  $V_{1\text{mA}}$ . In addition, the nonlinear exponent ( $\alpha$ ) was determined from  $\alpha = (\log J_2 - \log J_1)/(\log E_2 - \log E_1)$ , where  $J_1 = 1.0$  mA/cm<sup>2</sup>,  $J_2 = 10$  mA/cm<sup>2</sup>, and  $E_1$  and  $E_2$  are the electric fields corresponding to  $J_1$  and  $J_2$ , respectively.

The capacitance-voltage (C-V) characteristics of varistors were measured at 1 kHz using a RLC meter (QuadTech 7600) and an electrometer (Keithley 617). The donor concentration ( $N_d$ ) and the barrier height ( $\phi_b$ ) were determined by the equation  $(1/C_b - 1/C_{b0})^2 = 2(\phi_b + V_{gb})/q\varepsilon N_d$  [11], where  $C_b$  is the capacitance per unit area of a grain boundary,  $C_{b0}$  is the value of  $C_b$  when  $V_{gb} = 0$ ,  $V_{gb}$  is the applied voltage per grain boundary,  $q$  is the electronic charge,  $\varepsilon$  is the permittivity of ZnO ( $\varepsilon = 8.5\varepsilon_0$ ). The density of interface states ( $N_t$ ) at the grain boundary was determined by the equation  $N_t = (2\varepsilon N_d \phi_b / q)^{1/2}$  [11] and the depletion layer width ( $t$ ) of the either side at the grain boundaries was determined by the equation  $N_d t = N_t$  [12].

The microstructure was examined by a scanning electron microscope (SEM, Hitachi S2400). The average grain size ( $d$ ) was determined by the lineal intercept method [13]. The crystalline phases were identified by an X-ray diffractometry (XRD, Rigaku D/max 2100, Japan) with Cu K $\alpha$  radiation. The density ( $\rho$ ) of ZPCCD-based ceramics was measured by the Archimedes method.

Fig. 1 shows SEM micrographs of ZPCCD-based ceramics with Dy<sub>2</sub>O<sub>3</sub> content. SEM micrographs clearly show the influence of Dy<sub>2</sub>O<sub>3</sub> incorporation on the density and grain size. The sintered microstructure was less densified due to increasing porosity as Dy<sub>2</sub>O<sub>3</sub> content increases. The density of ceramics was decreased gradually from 5.53 to 4.43 g/cm<sup>3</sup> corresponding to 95.7–76.6% of theoretical density (TD = 5.78 g/cm<sup>3</sup> in ZnO). The average ZnO grain size was saliently decreased in the range of 18.6–4.7  $\mu\text{m}$  with increasing Dy<sub>2</sub>O<sub>3</sub> content. The decrease of grain size is attributed to the precipitation of secondary phase in the grain boundaries and nodal points.

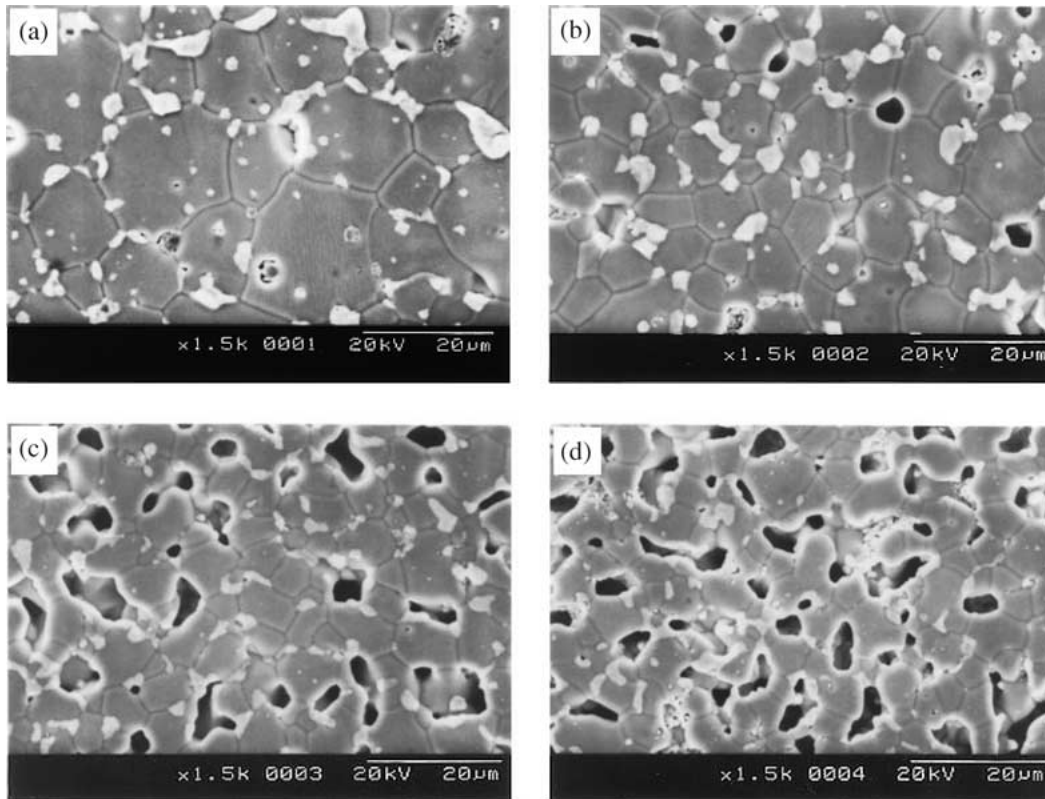


Figure 1 SEM micrographs of ZPCCD-based ceramics with  $\text{Dy}_2\text{O}_3$  content: (a) 0.0 mol%, (b) 0.5 mol%, (c) 1.0 mol%, and (d) 2.0 mol%.

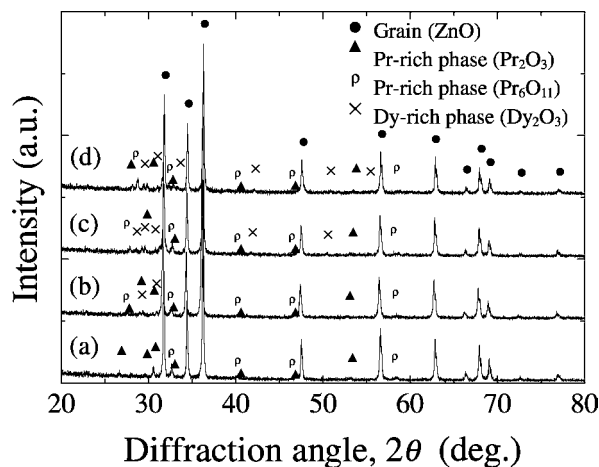


Figure 2 XRD patterns of ZPCCD-based ceramics with  $\text{Dy}_2\text{O}_3$  content: (a) 0.0 mol%, (b) 0.5 mol%, (c) 1.0 mol%, and (d) 2.0 mol%.

Fig. 2 shows the XRD patterns of ZPCCD-based ceramics with  $\text{Dy}_2\text{O}_3$  content. All varistor ceramics have only two phases, i.e., ZnO grain and intergranular layer, as revealed in the former work [7, 10]. Intergranular layer was composed of  $\text{Pr}_6\text{O}_{11}$  (or  $\text{Pr}_2\text{O}_3$ ) and  $\text{Dy}_2\text{O}_3$  and identified by EDS analysis to coexist in the grain boundaries and the nodal points. These phases could be indicated to SEM micrographs. The detailed microstructural parameters are summarized in Table I.

Fig. 3 shows the  $E$ - $J$  characteristics of ZPCCD-based varistors with  $\text{Dy}_2\text{O}_3$  content. It can be seen that the knee region of  $E$ - $J$  curves with  $\text{Dy}_2\text{O}_3$  is much keener than that without  $\text{Dy}_2\text{O}_3$  and especially, for the varistors with 0.5 mol%  $\text{Dy}_2\text{O}_3$ . Clearly, the incorporation of  $\text{Dy}_2\text{O}_3$  greatly improved the nonlinear properties of varistors. The detailed  $V$ - $I$  characteristic

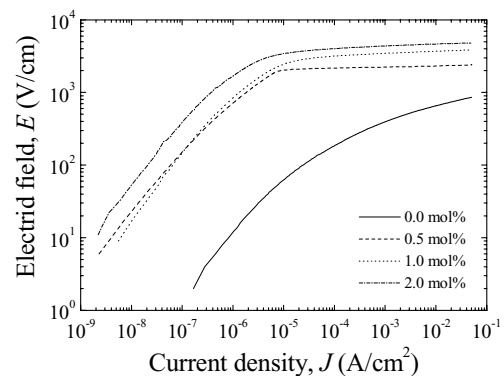


Figure 3  $E$ - $J$  characteristics of ZPCCD-based varistors with  $\text{Dy}_2\text{O}_3$  content.

parameters were summarized in Table I. The varistor voltage ( $V_{1\text{mA}}$ ) was greatly increased in the range of 39.4–436.6 V/mm. This is attributed to the increase of the number of grain boundaries due to the decrease of ZnO grain size with increasing  $\text{Dy}_2\text{O}_3$  content. The breakdown voltage per grain boundaries ( $V_{\text{gb}}$ ) was in the range of 2–3 V/gb in the varistors with  $\text{Dy}_2\text{O}_3$ , but the  $V_{\text{gb}}$  of varistor without  $\text{Dy}_2\text{O}_3$  was only 0.7 V/gb.

TABLE I Microstructural and  $V$ - $I$  characteristic parameters of ZPCCD-based varistors

$\text{Dy}_2\text{O}_3$ content (mol%)	$d$ ( $\mu\text{m}$ )	$\rho$ ( $\text{g}/\text{cm}^3$ )	$V_{1\text{mA}}$ (V/mm)	$V_{\text{gb}}$ (V/gb)	$\alpha$	$I_L$ ( $\mu\text{A}$ )
0.0	18.6	5.53	39.4	0.7	4.5	87.9
0.5	11.5	5.43	223.8	2.6	66.6	1.2
1.0	6.8	4.64	345.4	2.3	34.2	3.7
2.0	4.7	4.43	436.6	2.1	37.0	2.4

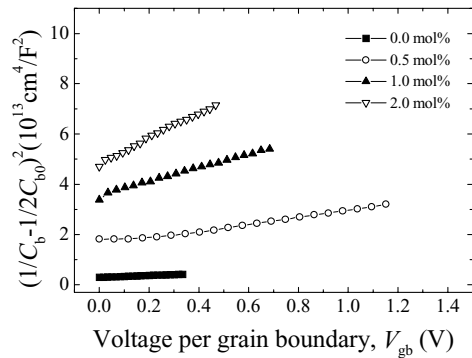


Figure 4 C-V characteristics of ZPCCD-based varistors with Dy<sub>2</sub>O<sub>3</sub> content.

Therefore, it is assumed that the ZPCC-based varistor without Dy<sub>2</sub>O<sub>3</sub> has poor grain boundaries.

The  $\alpha$  value in varistors without Dy<sub>2</sub>O<sub>3</sub> was only 4.5, whereas the  $\alpha$  value of the varistors with Dy<sub>2</sub>O<sub>3</sub> was abruptly increased above 30. Then, the  $\alpha$  value varied from maximum (66.6) in 0.5 mol% Dy<sub>2</sub>O<sub>3</sub> to minimum (34.2) in 1.0 mol% Dy<sub>2</sub>O<sub>3</sub>. The maximum  $\alpha$  value is much higher than that for incorporation of Er<sub>2</sub>O<sub>3</sub> and Y<sub>2</sub>O<sub>3</sub> reported previously in equivalent conditions [7, 10]. The  $I_L$  value in varistors without Dy<sub>2</sub>O<sub>3</sub> was 87.9  $\mu$ A, whereas the  $I_L$  value of the varistors with Dy<sub>2</sub>O<sub>3</sub> was very abruptly decreased below 4  $\mu$ A. The minimum value of  $I_L$  was obtained from 0.5 mol% Dy<sub>2</sub>O<sub>3</sub>, exhibiting 1.2  $\mu$ A. The variation of  $I_L$  value revealed to be opposite to that of  $\alpha$  value. As a result, the incorporation of Dy<sub>2</sub>O<sub>3</sub> was confirmed to significantly improve the nonlinear properties.

The capacitance-voltage ( $C$ - $V$ ) characteristics of ZPCCD-based varistors with Dy<sub>2</sub>O<sub>3</sub> content are shown in Fig. 4. It can be forecasted that Dy<sub>2</sub>O<sub>3</sub> greatly affects  $C$ - $V$  characteristics from the line slope and distribution. The detailed  $C$ - $V$  characteristic parameters were summarized in Table II. It was found that the increase of Dy<sub>2</sub>O<sub>3</sub> content leads to the decrease of the donor concentration ( $N_d$ ) from  $4.19 \times 10^{18}$  to  $0.33 \times 10^{18}/\text{cm}^3$  as well as the decrease of density of interface states ( $N_t$ ) from  $5.38 \times 10^{12}$  to  $1.74 \times 10^{12}/\text{cm}^2$ . Therefore, Dy<sub>2</sub>O<sub>3</sub> serves as an acceptor. The increase of the depletion layer width ( $t$ ) is attributed to the decrease of donor concentration. Really, the  $t$  is wider at side of lower doping region. With increasing Dy<sub>2</sub>O<sub>3</sub> content, the barrier height ( $\phi_b$ ) was increased up to

TABLE II C-V characteristic parameters of ZPCCD-based varistors

Dy <sub>2</sub> O <sub>3</sub> content (mol%)	$N_d$ ( $10^{18}/\text{cm}^3$ )	$N_t$ ( $10^{12}/\text{cm}^2$ )	$\Phi_b$ (eV)	$t$ (nm)
0.0	4.19	5.38	0.74	12.9
0.5	1.15	3.40	1.07	29.5
1.0	0.60	2.68	1.28	44.8
2.0	0.33	1.74	0.97	52.3

1.0 mol% and thereafter decreased. The  $\phi_b$  is directly connected with the  $N_d$  and  $N_t$ . In other words, the  $\phi_b$  is estimated by the variation rate in the  $N_t$  and  $N_d$ . In general, the  $\phi_b$  increases with increasing  $N_t$  and decreasing  $N_d$ .

### Acknowledgments

This work was supported by EEC (Electronic Ceramics Center) at Dongeui University as RRC. TIC program through KOSEF (Korea Science and Engineering Foundation), ITEP (Korea Institute of Industrial Technology Evaluation and Planning), and Busan Metropolitan City.

### References

1. L. M. LEVINSON and H. R. PILIPP, *Amer. Ceram. Soc. Bull.* **65** (1986) 639.
2. T. K. GUPTA, *J. Amer. Ceram. Soc.* **73** (1990) 1817.
3. Y. S. LEE and T. Y. TSENG, *ibid.* **75** (1992) 1636.
4. A. B. ALLES and V. L. BURDICK, *J. Appl. Phys.* **70** (1991) 6883.
5. Y.-S. LEE, K.-S. LIAO and T.-Y. TSENG, *J. Amer. Ceram. Soc.* **79** (1996) 2379.
6. C.-W. NAHM, H.-S. YOON and J.-S. RYU, *J. Mater. Sci. Lett.* **20** (2001) 393.
7. C.-W. NAHM, *Mater. Lett.* **47** (2001) 182.
8. *Idem.*, *J. Mater. Sci. Lett.* **21** (2002) 201.
9. C.-W. NAHM and B.-C. SHIN, *J. Mater. Sci.: Mater. Electro.* **12** (2002) 111.
10. C.-W. NAHM, *Mater. Lett.* **57** (2003) 1317.
11. M. MUKAE, K. TSUDA and I. NAGASAWA, *J. Appl. Phys.* **50** (1979) 4475.
12. L. HOZER, "Semiconductor Ceramics: Grain Boundary Effects" (Ellis Horwood, 1994) p. 22.
13. J. C. WURST and J. A. NELSON, *J. Amer. Ceram. Soc.* **55** (1972) 109.

Received 15 July  
and accepted 29 July 2003